Proceedings World Geothermal Congress 2020+1
Reykjavik, Iceland, April - October 2021

Numerical Analysis of Influencing Factors on Fast Water-Steam Transient in Geothermal Process

Xinzhe Zhao, Huilin Xing

School of Earth and Environmental Sciences, The University of Queensland, St Lucia 4072 Australia

Xinzhe.zhao@uqconnect.edu.au

Keywords: Phase change behavior, water-steam two phase flow, finite element method

ABSTRACT

In geothermal process, the fluid is often boiling or near boiling, and the flow may be either a two phase flow with a varying liquid saturation or a near boiling liquid which flashes to steam. This presents a substantial potential for geothermal hazards including steam kick or blowout in geothermal drilling and hydrothermal outburst in mining. However, previous works focus on the simulation of long-term geothermal process with phase change, the fast water-steam transient is less understood due to its high nonlinearity.

In this paper, based on pressure and enthalpy, the governing equations in the form of coupled nonlinear partial differential equations are formulated for describing multiphase flow in porous media. The IAPWS Industry Formulation 1997 formulation is used here to calculate water-steam thermodynamic properties and its derivatives in terms of pressure and enthalpy. A Newton-Raphson based nonlinear finite element technique is applied to solve the coupled highly nonlinear equations. Sudden changes of pressure and temperature in the geothermal process is simulated to address how water-steam transient is initiated. In addition, several important parameters, such as intrinsic permeability, porosity, rock density and rock heat capacity, which influence two phase fluid and heat flow in porous media are analyzed. The pressure, temperature, enthalpy and water saturation profiles are compared to figure out the controlling factor of fast water-steam transient behavior.

Results from this numerical simulation work are helpful to understand the water-steam transient behavior in geothermal process, and it also has guiding significance for geothermal hazards prediction.

1. INTRODUCTION

Fluid and heat flow accompanied by a water-steam phase change in porous media has gained an increasing importance in a variety of scientific and engineering applications. The areas of application include oil thermal recovery(Coats, George et al. 1974, Bergins, Crone et al. 2005), oil-shale retorting, thermal energy storage(Zalba, Marın et al. 2003), nuclear waste disposal (Doughty, Pruess et al. 1988)and geothermal systems(Shaik, Rahman et al. 2011, Xing 2014, Croucher, O'Sullivan et al. 2018).Particularly, in a geothermal system, due to large changes in temperature and pressure, water steam phase change may occur during the process of fluids flow. The fluid flow may be either steam and water flow with a varying liquid saturation or a near-boiling liquid which flashes to steam(O'Sullivan 1981, Croucher, O'Sullivan et al. 2016). Water-steam phase change behavior is not only recognized in geothermal energy extraction, but also in geothermal drilling and mining. When drilling in an aquifer confined between two impermeable rock layers, the sudden depressurization will cause a self-vaporization of the water, which presents a substantial potential for geothermal hazards including steam kick and hydrothermal outburst(Melaku 2005, Singh 2010).

In the publication of fluid and heat flow in porous medium reviewed, there are many traits in common. In general, a mathematical description of fluid and heat flow based on mass, energy and momentum (Darcy's equation is a simplified momentum balance) balances is developed first, and those balance equations are reduced to two nonlinear partial differential equations in terms of the unknown dependent variables. For single phase flow problem, pressure and temperature are generally used as the independent variables. However, when two phase flow happen, pressure and temperature are not independent variables any more. In order to simulate both single and two phase flow, several choices of the independent variables have been made by several researchers: pressure and enthalpy(p, h)(Witherspoon, Neuman et al. 1975, Faust 1976), density and internal energy(ρ, u)(Garg, Blake et al. 1975, Garg, Pritchett et al. 1978), pressure, temperature and saturation(p, T, S_w)(Thomas and Pierson 1978, Croucher, O'Sullivan et al. 2018).

Over the years, considerable effort has been made to develop computer simulations of both heat and mass transfer in porous media without phase change behaviors. Those studies are mostly concerned with free convection and neglect viscous dissipation and compressible work. In fact, the literature of numerical simulation of water-steam flows coupled with heat flow with an accompanying phase change is comparatively limited. Simulating transient two phase coupled geothermal flow dynamics with phase change behavior is difficult due to its highly nonlinear coupling process. This is because mass exchange occurs between water and steam phase with large density ratio ($\approx$1000) during phase change process. Also, the numerical method for such problems needs to account for incompressible (water) and compressible (steam) in the same computational domain. Due to the strongly nonlinearity nature of governing equations and constitutive equations, in the numerical solution for these hyperbolic equations, numerical oscillation occurs within the progress of computation, which is unacceptable because oscillations can be greatly amplified as iterations continue. Also, discontinuities in the thermo-physical properties of fluid at the phase boundaries pose a great challenge which induces limitations on time step size. It is reported that to solve this difficulty in computing phase change, all functions of thermodynamic variables in governing equations should be numerically continuous across the phase boundaries, even if derivatives of those functions can change by several orders of magnitude(Voss 1979).

In the numerical simulation of geothermal reservoirs involves nonlinear phase transitions, there is no universally accepted numerical techniques for establishing relative accuracy and stability. Finite difference and Galerkin finite element method are commonly used. Toronyi & Farouq Ali (1975) developed a two-phase, two-dimensional finite-difference geothermal simulator Coupled with a wellbore model. The mass and energy balance equations were solved by an IMPES formulation. Since they used pressure and saturation as dependent variables, their model was restricted to two phase fluid flow. Lesseter et al. (1975) formulated their mass and energy couple equations describing a one or two phase fluid flow in porous media for transient or steady state, in which internal energy and density are the dependent variables. Their model is capable of modeling one, two and three dimensional problems. Integrated finite difference technique was used to for discretization and then the equations were solved semi- implicitly for discrete time steps. Coats (1977) proposed a three dimensional transient model for single or two phase flow based on pressure, temperature and saturation formulation. Finite difference method was used in conjunction with fully implicit Newton-Raphson iteration. Developed at Lawrence Berkeley National Laboratory (LBNL) of the U.S. Department of Energy (DOE), TOUGH2 has been used extensively in geothermal resource. It is based on as integrated finite difference numerical method for non-isothermal flows of multiphase, multicomponent fluid and heat flow with phase change.(Horne and O'Sullivan 1977, Pruess and Narasimhan 1982, Mannington, O'Sullivan et al. 2004). For single phase state, pressure and temperature are treated as dependent variables, when phase change happen, the primary variables are switched from pressure and temperature to pressure and saturation.

Since compared with finite difference method, finite element method is more realistic for it great flexibility in dealing with large structures and irregular geometries and its high computational efficiency. In some papers, finite element method was also employed to obtain approximate solutions. Faust &Mercer (1975) applied both finite difference and Galerkin finite element method to develop a two phase geothermal model in two horizontal dimensions based on pressure enthalpy formulation. For single phase flow, the finite element method was more attractive than finite difference method. For two phase flow, the oscillations can be reduced in finite difference mode by upstream weighting procedure. But unfortunately, this procedure didn't work for finite element model. In 1978, Huyakorn &Pinder employed a new Galerkin finite element techniques to reduce the numerical oscillations. In this new finite element method, asymmetric weighing functions were used and a modified Newton-Raphson method was applied for dealing with nonlinear coefficients. The finite element heat and mass (FEHM) transfer simulator, developed at Los Alamos National Laboratory is a strong two-phase porous medium model. By the control-volume finite element method, it can simulate 2-D and 3-D non-isothermal, multiphase and multi-component heat and fluid flow both in porous and facture medium. While with the governing equation based on pressure and temperature, it is difficult to model phase change behavior(Zyvoloski, Robinson et al. 1997).

Previous related research focused on long-term geothermal process. However, due to its highly nonlinear coupling behavior ,the phase change in transient geothermal process is less understood and remains great challenging for both modeling and computer computation. It has received more and more attention in recent years and is still the subject of intensive ongoing research. In this paper, a new simulation code for transient water-steam phase change behavior considering water properties as functions of pressure and enthalpy is developed. The latest IAPWS Industry Formulation 1997 is used as precise algorithms for calculating fluid properties in water and water-steam region. The nonlinearities and slope discontinuities in the governing equations are presented in great details and the numerical technique of dealing with nonlinearity is also proposed here.

2. MATHEMATICAL FORMULATION

The mathematical model used in this paper is based on balance equations for mass and energy of each phase in porous media. With the assumption of thermal equilibrium between fluid and rock, those conservation equations are combined and can be expressed as(Faust and Mercer 1979),where the subscript s is for steam, w is for water, and r is for rock:

$$\frac{\partial(\phi\rho)}{\partial \mathrm{t}} + \nabla\cdot(\rho_s v_s) + \nabla\cdot(\rho_w v_w) = 0 \tag{1}$$

$$\frac{\partial[\phi\rho \mathrm{h} + (1-\phi)\rho_r h_r]}{\partial \mathrm{t}} + \nabla\cdot(\rho_s h_s v_s) + \nabla\cdot(\rho_w h_w v_w) - \nabla\cdot(k_m \nabla T) = 0 \tag{2}$$

where ρ is density of the total steam-water mixture, defined as:

$$\rho = S_w\rho_w + S_s\rho_s \tag{3}$$

h is enthalpy of the total steam-water mixture, defined as:

$$\mathrm{h} = (S_s\rho_s h_s + S_w\rho_w h_w)/\rho \tag{4}$$

where ϕ is the porosity;S is the phase saturation, $S_w + S_s = 1$; h is the specific enthalpy,J/kg;ρ is density, kg/m^3; υ is fluid flow rate,$\mathrm{kg}\cdot s^{-1}\cdot m^{-2}$; κ_m is the effective heat conductivity of rock and fluid, ,$\mathrm{W}/(\mathrm{m}\cdot ℃)$;T is temperature,℃.

For momentum balance equations, Darcy's equation is used as a simplified momentum balance for modelling multiphase flow. Here, capillarity and gravity are neglected.

$$v_w = -\frac{k k_{rw}}{\mu_w}\nabla p \tag{5}$$

$$v_s = -\frac{k k_{rs}}{\mu_s}\nabla p \tag{6}$$

where p is fluid pressure,pa; k is the intrinsic permeability of porous medium,m^2;k_{rw} and k_{rs} are the relative permeability of water and steam , m^2;μ is the dynamic viscosity,pa · s;

By substituting Equation (5) and (6) into Equation (1) and (2) , the following governing equations can be obtained:

$$\frac{\partial(\phi\rho)}{\partial \mathrm{t}} - \nabla \cdot [(\frac{kk_{rs}\rho_s}{\mu_s} + \frac{kk_{rw}\rho_w}{\mu_w})\nabla p] = 0 \tag{7}$$

$$\frac{\partial[\phi\rho \mathrm{h} + (1-\phi)\rho_r h_r]}{\partial \mathrm{t}} - \nabla \cdot [(\frac{kk_{rs}\rho_s h_s}{\mu_s} + \frac{kk_{rw}\rho_w h_w}{\mu_w})\nabla \mathrm{p}] - \nabla \cdot (k_m \nabla T) = 0 \tag{8}$$

3. THERMODYNAMIC OF WATER

The equations of thermodynamic properties of pure water and steam adopted in this paper is IAPWS-IF97 Formulation(Wagner and Kretzschmar 2007) . Compared with IFC-67 and IAPWS-95, it has significantly improved both accuracy and calculation speed. IAPWS-IF97 is preferable when the computational speed is a major consideration, for example, in calculation involving finite element methods. Figure 1 shows five thermodynamic regions in a pressure-enthalpy diagram of IAPWS-IF97 Formulation, in which region 1 in compressed water, region 2 is superheated steam, region 3 is supercritical region, region 4 is two phase region and region 5 is high-temperature region.

In this paper, total density (ρ), water /steam densities (ρ_w ,ρ_s), water saturation (s_w), viscosity (μ_w , μ_s) and temperature (T) are considered functions of pressure and enthalpy. Porosity is a function of pressure, which means taking solid compressibility into consideration. When the state of fluid lies in the two-phase region, the intrinsic properties of water and steam (ρ_w ,ρ_s, μ_w , μ_s ,h_w and h_s) are only dependent on the pressure.

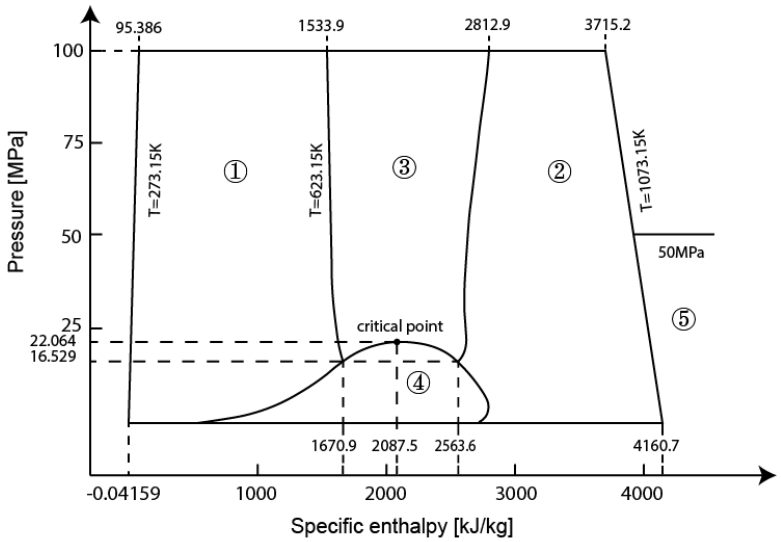

Figure 1 Regions and region boundaries of IAPWS-IF97 for the variables (p, h)

Fluid thermodynamic properties are determined from IAPWS-IF97, and by employing the chain rule, the governing equations (7) and (8) can be written in the reduced parameter form:

$$C^P \frac{\partial p}{\partial t} + C^H \frac{\partial h}{\partial t} = \nabla \cdot (\tau \nabla p) \tag{9}$$

$$D^P \frac{\partial p}{\partial t} + D^H \frac{\partial h}{\partial t} = \nabla \cdot (\lambda \nabla p) + \nabla \cdot (\beta \nabla h) \tag{10}$$

where C^P ,C^H, D^P ,D^H, τ, λ, β are the seven nonlinear coefficients defined as follows:

$$C^P = \rho \frac{d\phi}{dp} + \phi(\frac{\partial \rho}{\partial p})_h \tag{11a}$$

$$C^H = \phi \left(\frac{\partial \rho}{\partial h}\right)_p \tag{11b}$$

$$D^P = (\rho h - \rho_r h_r)\frac{\mathrm{d}\phi}{\mathrm{dp}} + \phi h \left(\frac{\partial \rho}{\partial p}\right)_h + (1-\phi)\rho_r \frac{dh_r}{dT}\left(\frac{\partial T}{\partial p}\right)_h \tag{11c}$$

$$D^H = \phi h \left(\frac{\partial \rho}{\partial h}\right)_p + \phi\rho + (1-\phi)\rho_r \frac{dh_r}{dT}\left(\frac{\partial T}{\partial h}\right)_p \tag{11d}$$

$$\tau = \frac{kk_{rs}\rho_s}{\mu_s} + \frac{kk_{rw}\rho_w}{\mu_w} \tag{11e}$$

$$\lambda = \mathrm{k}\left(\frac{\rho_s h_s k_{rs}}{\mu_s} + \frac{\rho_w h_w k_{rw}}{\mu_w}\right) + \kappa_m \left(\frac{\partial T}{\partial p}\right)_h \tag{11f}$$

$$\beta = \kappa_m \left(\frac{\partial T}{\partial h}\right)_p \tag{11g}$$

The relative permeabilities of water and steam used in this paper is Corey model, which is one of the most commonly used relative permeability functions for simulations of water-steam flow in porous medium (Corey 1954, Horne, Satik et al. 2000, Gudjonsdottir, Palsson et al. 2015).The Corey model is expressed as follows:

$$k_{rl} = S_l^{*4} \tag{12a}$$

$$k_{rv} = (1 - S_l^*)^2\left(1 - S_l^{*2}\right) \tag{12b}$$

$$S_l^* = (S_l - S_{lr})/(1 - S_{lr} - S_{vr}) \tag{12c}$$

where S_{lr} and S_{vr} are the irreducible saturation for liquid and vapor and it is common to assume S_{lr} and S_{vr} to be 0.3 and 0.05,respectively.

The variation of these non-linear coefficients with pressure and enthalpy are presented in Figure 2 and Figure 3 respectively. It is clear that at the boundary between the water and two phase regions, the nonlinear coefficients display a sharp change. The drastic changes of the properties when phase change occurs will cause a major convergence difficulty in the numerical simulation of water-steam flow in porous medium.

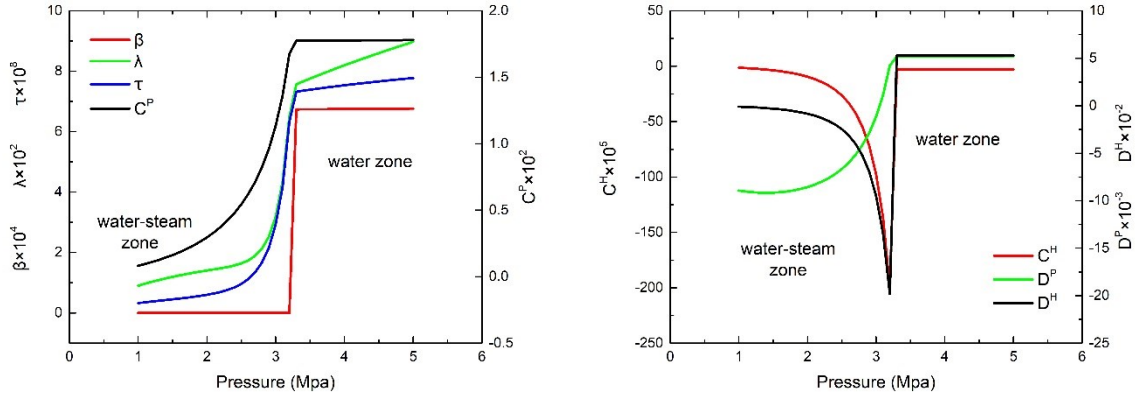

Figure 2 variation of nonlinear coefficients with constant enthalpy (h=1028kJ/kg)

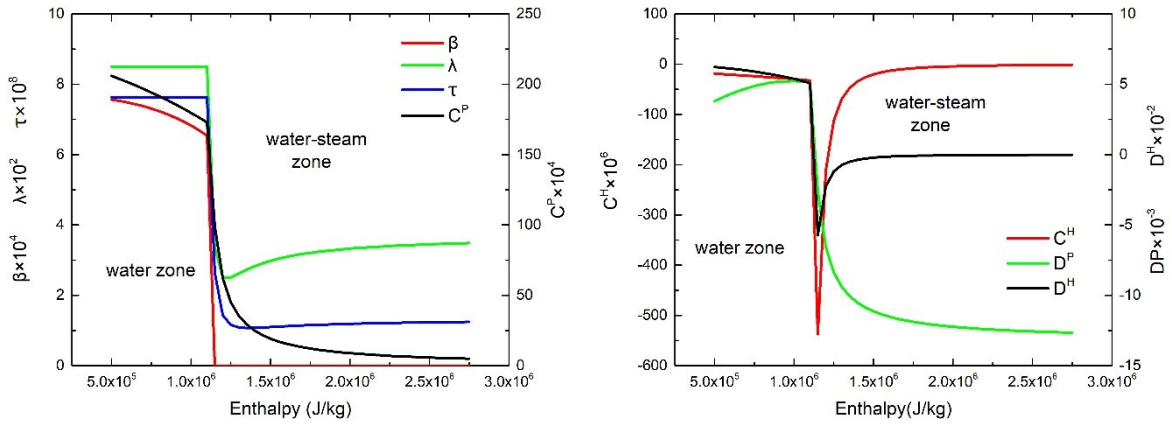

Figure 3 variation of nonlinear coefficients with constant pressure (p=4.38Mpa)

4. NUMERICAL IMPLEMENTATION

The finite element method is used to discretize the nonlinear partial differential Equations (9) and (10).First, the spatial discretization will be discretized by a general weighted residual method, and then a semi-implicit differencing method will be used for time discretization. Compared with the explicit differencing method, second-order semi-implicit differencing method improves the solution accuracy. After space and time discretization, a set of nonlinear algebraic equation will be obtained which is solved by

Newton-Raphson iterative method. To ensure the numerical stability, automatic time step control and three convergence criterions are used here.

4.1 Equation discretization

To solve the above governing equations, the approximation of the pressure and enthalpy over the each element can be written as

$$p(x_i\ ,t) \cong \hat{p}(x_i\ ,t) = N_J(x_i)p_J(t) \tag{13}$$

$$h(x_i\ ,t) \cong \hat{h}(x_i\ ,t) = N_J(x_i)h_J(t) \tag{14}$$

where ($\hat{}$) denotes a discretized function, $N_J(x_i)$ denotes the shape functions, $p_J(t)$ and $h_J(t)$ denote nodal value of pressure and enthalpy at time t .Cartesian coordinates x, y, z are indicated by x_i concisely.

Let W_I be a set of weighting functions and the governing equations can be discretized by weighted residual method:

$$\int_V W_I \frac{\partial}{\partial x_i}\left(\tau \frac{\partial \hat{p}}{\partial x_i}\right) dV = \int_V N_I C^P \frac{\partial \hat{p}}{\partial t} dV + \int_V N_I C^H \frac{\partial \hat{h}}{\partial t} dV \tag{15}$$

$$\int_V W_I \frac{\partial}{\partial x_i}\left(\lambda \frac{\partial \hat{p}}{\partial x_i}\right) dV + \int_V W_I \frac{\partial}{\partial x_i}\left(\beta \frac{\partial \hat{h}}{\partial x_i}\right) dV = \int_V N_I D^P \frac{\partial \hat{p}}{\partial t} dV + \int_V N_I D^H \frac{\partial \hat{h}}{\partial t} dV \tag{16}$$

where V is the domain over which the integration is performed. Employing integration by parts and Green's theorem on the second derivative terms, Equation (15) and Equation (16) can be written as:

$$\int_V W_I \tau \frac{\partial \hat{p}}{\partial x_i}\frac{\partial W_I}{\partial x_i} dV + \int_V N_I C^P \frac{\partial \hat{p}}{\partial t} dV + \int_V N_I C^H \frac{\partial \hat{h}}{\partial t} dV - \int_S W_I \tau \frac{\partial \hat{p}}{\partial x_i} n_i\, dS = 0 \tag{17}$$

$$\int_V W_I \lambda \frac{\partial \hat{p}}{\partial x_i}\frac{\partial W_I}{\partial x_i} dV + \int_V W_I \beta \frac{\partial \hat{h}}{\partial x_i}\frac{\partial W_I}{\partial x_i} dV + \int_V N_I D^p \frac{\partial \hat{p}}{\partial t} dV + \int_V N_I D^H \frac{\partial \hat{h}}{\partial t} dV - \int_S W_I \lambda \frac{\partial \hat{p}}{\partial x_i} n_i\, dS - \int_S W_I \beta \frac{\partial \hat{h}}{\partial x_i} n_i\, dS = 0 \tag{18}$$

where S is the boundary of the domain is, n_i is the outward unit normal vector on the boundary. For presenting the numerical procedure, we drop the boundary integral terms of Equation (17) and Equation (18) to get:

$$\int_V W_I \tau \frac{\partial \hat{p}}{\partial x_i}\frac{\partial W_I}{\partial x_i} dV + \int_V N_I C^P \frac{\partial \hat{p}}{\partial t} dV + \int_V N_I C^H \frac{\partial \hat{h}}{\partial t} dV = 0 \tag{19}$$

$$\int_V W_I \lambda \frac{\partial \hat{p}}{\partial x_i}\frac{\partial W_I}{\partial x_i} dV + \int_V W_I \beta \frac{\partial \hat{h}}{\partial x_i}\frac{\partial W_I}{\partial x_i} dV + \int_V N_I D^p \frac{\partial \hat{p}}{\partial t} dV + \int_V N_I D^H \frac{\partial \hat{h}}{\partial t} dV = 0 \tag{20}$$

Substitution of Equation (13) and (14) into Equation (19) and (20) leads to:

$$\int_V C^P N_I N_J\, dV \frac{\partial p_J}{\partial t} + \int_V C^H N_I N_J\, dV \frac{\partial h_J}{\partial t} + \int_V \tau W_I \frac{\partial N_J}{\partial x_i}\frac{\partial W_I}{\partial x_i} dV\, p_J = 0 \tag{21}$$

$$\int_V D^P N_I N_J\, dV \frac{\partial p_J}{\partial t} + \int_V D^H N_I N_J\, dV \frac{\partial h_J}{\partial t} + \int_V \lambda W_I \frac{\partial N_J}{\partial x_i}\frac{\partial W_I}{\partial x_i} dV\, p_J + \int_V \beta W_I \frac{\partial N_J}{\partial x_i}\frac{\partial W_I}{\partial x_i} dV\, h_J = 0 \tag{22}$$

Equation (21) and Equation (22) are semi-discrete as they are only discretized is space. The nonlinear coefficients change with the time, and the improper time discretization can result in inaccurate solutions. In this study, a semi-implicit scheme (Crank-Nicolson method) is used for the numerical evaluation in time domain. Then a system of nonlinear algebraic equations are accomplished as follow:

$$\left(A_{IJ} + \tfrac{1}{2}\Delta t C_{IJ}\right) p_J^{n+1} + B_{IJ} h_J^{n+1} = \left[A_{IJ} - \tfrac{1}{2}\Delta t C_{IJ}\right] p_J^n + B_{IJ} h_J^n \tag{23}$$

$$\left(D_{IJ} + \tfrac{1}{2}\Delta t F_{IJ}\right) p_J^{n+1} + \left(E_{IJ} + \tfrac{1}{2}\Delta t G_{IJ}\right) h_J^{n+1} = \left[D_{IJ} - \tfrac{1}{2}\Delta t F_{IJ}\right] p_J^n + \left[E_{IJ} - \tfrac{1}{2}\Delta t G_{IJ}\right] h_J^n \tag{24}$$

where

$$A_{IJ} = \int_V C^P N_I N_J\, dV \tag{25a}$$

$$B_{IJ} = \int_V C^H N_I N_J\, dV \tag{25b}$$

$$C_{IJ} = \int_V \tau W_I \frac{\partial N_J}{\partial x_i}\frac{\partial W_I}{\partial x_i} dV \tag{25c}$$

$$D_{IJ} = \int_V D^P N_I N_J\, dV \tag{25d}$$

$$E_{IJ} = \int_V D^H N_I N_J\, dV \tag{25e}$$

$$F_{IJ} = \int_V \lambda W_I \frac{\partial N_J}{\partial x_i}\frac{\partial W_I}{\partial x_i} dV \tag{25f}$$

$$G_{IJ} = \int_V \beta W_I \frac{\partial N_J}{\partial x_i}\frac{\partial W_I}{\partial x_i} dV \tag{25g}$$

This set of nonlinear equation with dependent variables pressure and enthalpy can be written in residual-rate form:

$$\boldsymbol{f}(\boldsymbol{u}) = 0 \tag{26}$$

where $\boldsymbol{f}$ is the vector of residual rates of Equation (23) and (24), $\boldsymbol{u}$ is the vector of unknown pressure and enthalpy

The Newton-Raphson method is used here solving:

$$[\boldsymbol{J}(\boldsymbol{u}_i)]\{\Delta \boldsymbol{u}_i\} + \{\boldsymbol{f}(\boldsymbol{u}_i)\} = 0 \tag{27}$$

$$\{\boldsymbol{u}_{i+1}\}=\{\boldsymbol{u}_i\} + \{\Delta \boldsymbol{u}_i\} \tag{28}$$

where $[\boldsymbol{J}(\boldsymbol{u}_i)]$is Jacobian matrix and i is the current equilibrium iteration. To get a converged solution, more than one Newton-Raphson iteration is needed:

1. Initiate the computation with initial guess of $\{\boldsymbol{u}_0\} = \{0\}$;

2 .Compute the updated Jacobian matrix and residue rate;

3. Calculate $\{\Delta \boldsymbol{u}_i\}$ from Equation (27) using one or two linear solver

4. Add $\{\Delta \boldsymbol{u}_i\}$ to $\{\boldsymbol{u}_i\}$ to get the next approximation $\{\boldsymbol{u}_{i+1}\}$

5. Repeat steps 2 to 4 until convergence is obtained.

4.2 Automatic time step control

Adaptive time step algorithm has a great impact on numerical computation stability and reliability. As can be seen in Figure 2 and Figure 3, the coefficients at the phase change boundary change rapidly, which requires automatic time step control to prevent numerical instabilities. In general, the faster the changes, the smaller time step is needed for computation stability and solutions accuracy.

The maximum allowable values for changes in pressure and enthalpy, and minimum acceptable time step are specified. Then,

$$DPMAX^n = max\{|\Delta p^n|\} \tag{29}$$

$$DHMAX^n = max\{|\Delta h^n|\} \tag{30}$$

if $DPMAX^n > 1.1DPLIM$ or if $DPMAX^n < 0.9DPLIM$, then

$$\Delta t_p^{n+1} = \Delta t^n \frac{DPLIM}{DPMAX^n} \tag{31}$$

$$\Delta t_h^{n+1} = \Delta t^n \frac{DHLIM}{DHMAX^n} \tag{32}$$

This algorithm will maintain pressure and enthalpy changes close to the limit value on maximum pressure and enthalpy change over the time step. However, the actual changes of dependent variables are not linear, the limiting values could be considerably exceed with an adjust time step. So the following constraint should be included:

$$\Delta t_{min} \le \Delta t^{n+1} \le f\Delta t^n \tag{33}$$

the new time step

$$\Delta t^{n+1} = min\{\Delta t_h, \Delta t_p \quad\} \tag{34}$$

When phase change occurs in certain time step, the following time step control is used to reduce the time step. If the number of phase change nodes is greater than the specified number of phase change nodes, the time step will be cut by the factor of $\alpha(0 < \alpha < 1)$, where $\alpha = max\left\{\frac{N_s}{N}, 0.5\right\}$. By multiplying α, the new time step is always greater or equal to the half of the current time step.

4.3 Convergence control

Three convergence criterions are used is this paper for determining convergence of the iterative procedures. The primary convergence criterion is that the L^2 norms of the fluid mass residual rates and the energy residual rates are less that the specified limits. The L^2 norm of a vector is the square root of the sum of the squares value of the terms. Boundary notes with specified pressure and enthalpy are not included in the convergence test because their residuals do not decrease as solution is approached.

The second convergence criterion, applied when phase change occurs in current step, is that the L^2 norms of the relative changes of pressure and enthalpy in an iteration are less than specified limits.

The third convergence criterion is not applied until after four iteration steps have been taken. The third convergence criterion is L^2 norm of the change in pressures is less than 1 kPa and the L^2 norm of the absolute change in enthalpy is less than 100J/kg.

5. MODEL DESCRIPTION

In this study, a concept model (Figure 4) is established for simulating sudden pressure and temperature change in the surface region of geothermal systems.

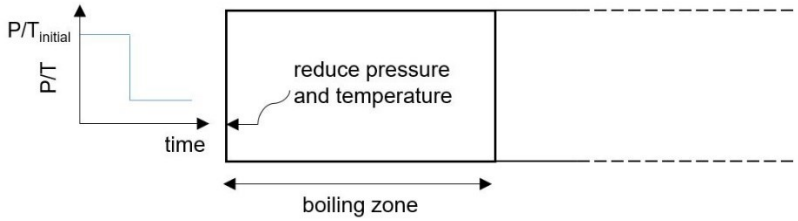

Figure 4 conceptual model for inducing phase change by pressure reduction

The initial pressure and temperature of this model are uniform,whick make sure that throughout the whol region the fluid is all-liquid state. The initial temperature is 220℃,which is the water/steam saturation temperature of 2.32 MPa ($T_{sat}(2.32Mpa) = 220\ ℃$). The initial pressure is 2.45 MPa, so the pressure drop 0.13MPa will cause fluid boiling. And other input paretmers are listed in Table 1

Table 1 Input parameters for numerical simulation

Parameters	value
Model geometry (m)	20×2×2
Initial pressure (MPa)	2.45
Initial temperature (℃)	220
Intrinsic permeability (m^2)	5×10^{-13}
Intrinsic porosity	0.08
Heat capacity of rock (J/kg℃)	930
Density of rock (kg/m^3)	2657
Thermal conductivity of rock (W/m ℃)	2.3

The sudden pressure and temperature change at the left face will induce water boil to the steam. The Figure 5 shows pressure, enthalpy, temperature and water saturation distribution at 92.08s. As can be seen in Figure 6, in the initial, the fluid near left face lies in the water region, and the sudden drop of pressure and temperature make it cross phase boundary to become water-steam flow.

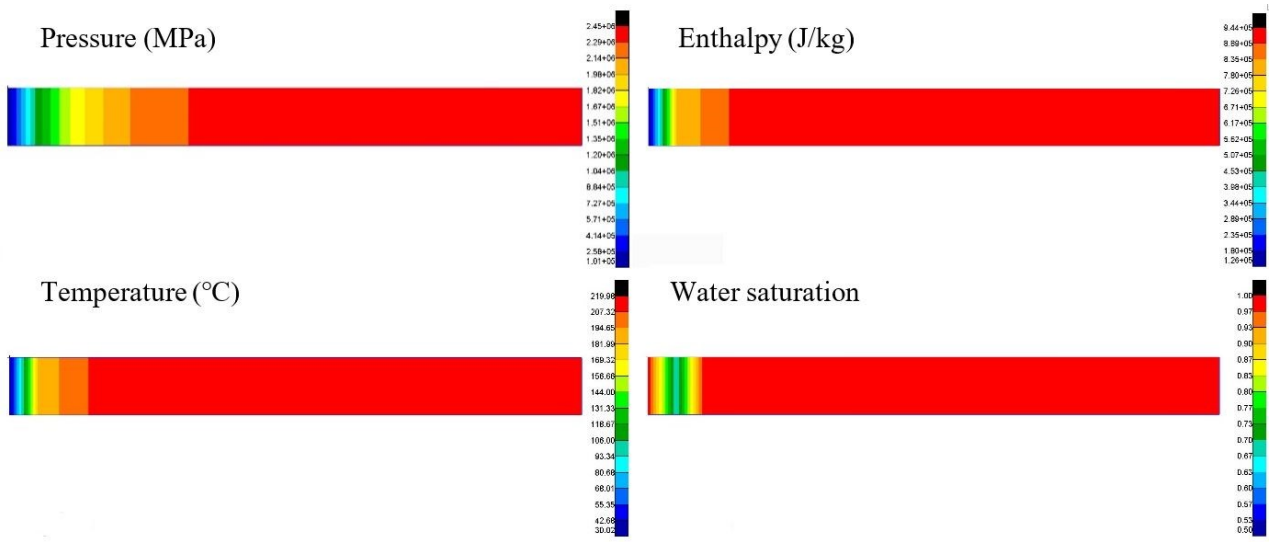

Figure 5 The pressure, enthalpy,temperature and water saturation at t=92.08s

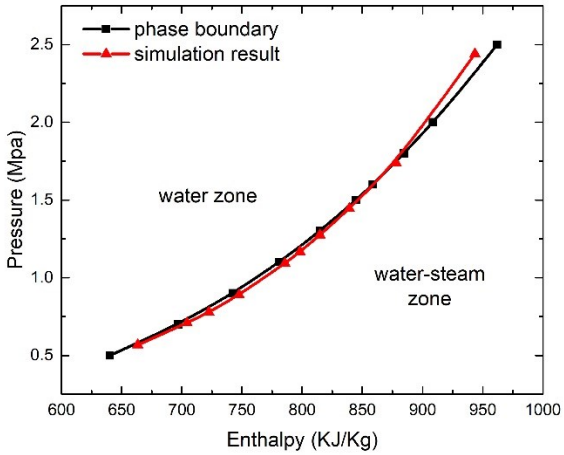

Figure 6 Pressure-enthalpy diagram of how water-steam phase change happen

6. RESEULT AND DISSCUSSION

In this paper, sensitivity analysis to the following parameters are conducted: the formation intrinsic permeability,k; formation intrinsic porosity,ϕ; rock heat capacity of rock,c_r; rock density, ρ.Based on the reference case, the following 4 scenarios are researched in span of 800s:(a) decreasing k to k =0.5×10^{-13}m^2; (b) increasing ϕ to ϕ=0.375; (c) greater rock density ρ=2827 kg/m^3 (d) greater rock heat capacity c_r=1170 J/kg℃. The pressure, temperature, enthalpy and water saturation profiles at x=1m are compared to investigate their effect on water-steam phase change evolution.

6.1 Influence of permeability

Figure 7 shows the pressure, enthalpy, temperature and water saturation profiles with different formation intrinsic permeability. It is clear that decreasing permeability from 5×10^{-13} m^2 to 0.5×10^{-13} m^2 has significant effect on pressure evolution. And enthalpy and temperature evolves with similar pattern as the pressure in total 800s. It is due to the fact that as permeability decreases the fluid flow in porous medium decreases and the heat transfer between rock and fluid therefore decreases. Since it has been demonstrated that heat transfer by fluid flow is the dominating factor in the thermal process in the porous medium. To sum up, formation intrinsic permeability has a pronounced effect on fluid and heat transfer in porous medium. The result here is in consistent with the typical geothermal systems.

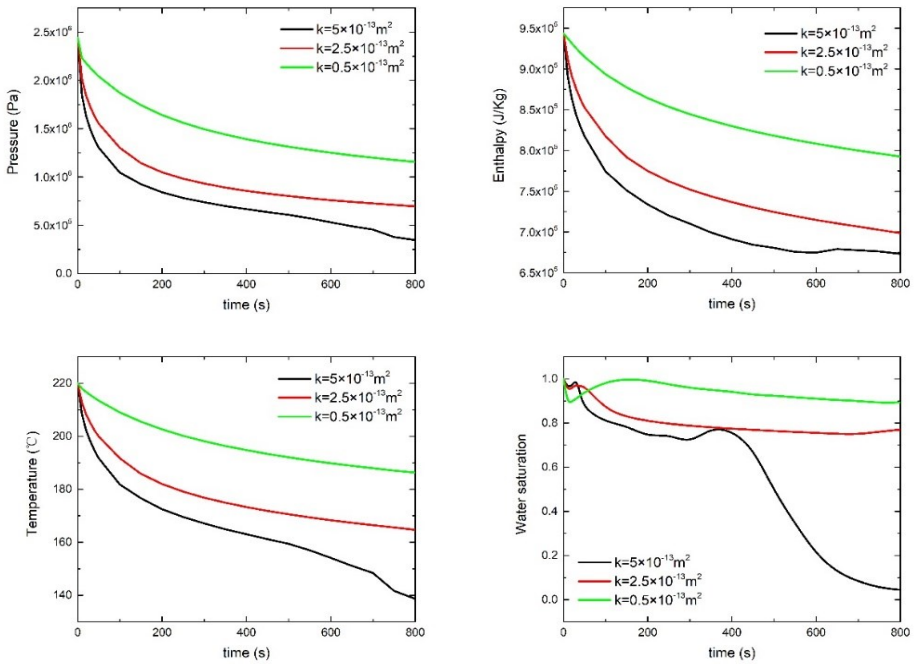

Figure 7 Pressure, enthalpy, temperature and water saturation with different permeability

6.2 Influence of porosity

The porosity is one of the important factors that can determine the initial heat of the formation. The lower porosity means higher volume of solid rock in the formation, and then higher amount heat can be conducted to the fluid. Since the intrinsic permeability is unchanged, increasing porosity has little effect on pressure decline. From the results of this study it can be observed that at the initial stage, the higher porosity is, the more steam is produced. Besides, for the high porosity (with porosity of 0.275 and 0.375) water saturation decreases first and then increases up to 1.0, which means at first water flashes to steam and then steam condensate to water again. The rate of steam condensate for high porosity is faster for low porosity. It can be concluded that the higher the porosity is, the more water is prone to boiling when sudden pressure drop happens.

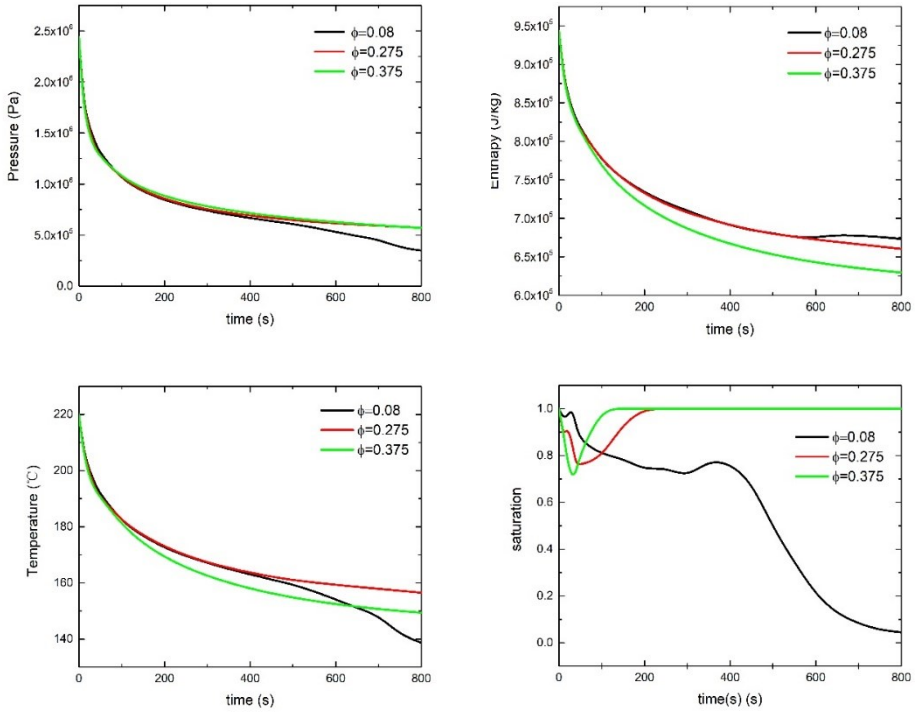

Figure 8 Pressure,enthalpy,temperature and water saturation with different porosity

6.3 Influence of rock density

According to the Debye-Equation (Eq.35), rock thermophysical properties are controlled by rock density(Sass and Götz 2012).

$$\rho_r = \frac{\kappa_r}{c_r \cdot \alpha} \tag{35}$$

where ρ_r is rock density, kg/m^3; κ_r is thermal conductivity of rock, $\mathrm{W}/(\mathrm{m} \cdot \mathrm{K})$; $c_r$is rock specific heat capacity, $\mathrm{J}/(\mathrm{kg} \cdot K)$; α is thermal diffusivity,m^2/s.

And density itself is closely related to the facies of the sedimentary rocks. So in this research, pressure, enthalpy, temperature and water saturation profiles are compared with different densities. In the Figure 9, we can see that in the initial, different rock density has little effect on the pressure, enthalpy, temperature and water saturation. As time goes on, more steam is produced with lower rock density. It can be deduced that a higher rock density means more heat stored in the formation, and more heat thermal energy in place can offset the heat loss led by fluid flow.

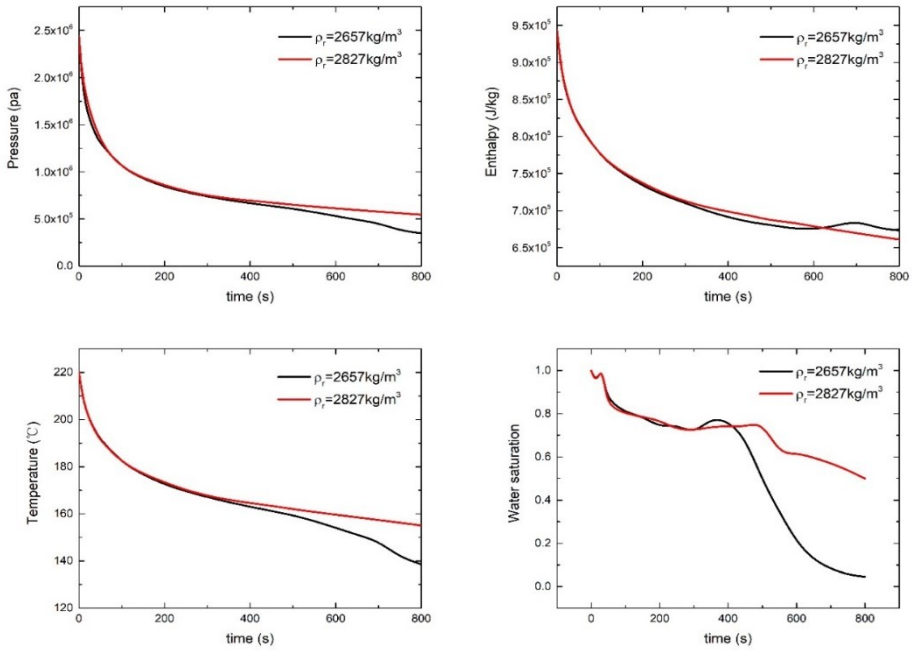

Figure 9 Pressure,enthalpy,temperature and water saturation with different rock density

6.4 Influence of rock heat capacity

With certain rock mass and its temperature, rock heat capacity determines how much thermal energy is stored in the formation. The higher the heat capacity means the greater thermal inertia, therefore it is more difficult to change the temperature with higher heat capacity, which has been shown in the temperature profile in Figure 10.As we can see from Figure 10, in the first 400s, different rock heat capacity has little effect on the pressure, enthalpy, temperature and water saturation evolution. As time goes on, more water flashes to the steam with lower rock heat capacity. A decrease in pressure can result in a phase change from water to the steam, and fluid flow induced by pressure decline can lead to heat loss. Higher heat capacity will prevents heat loss, so little steam is achieved.

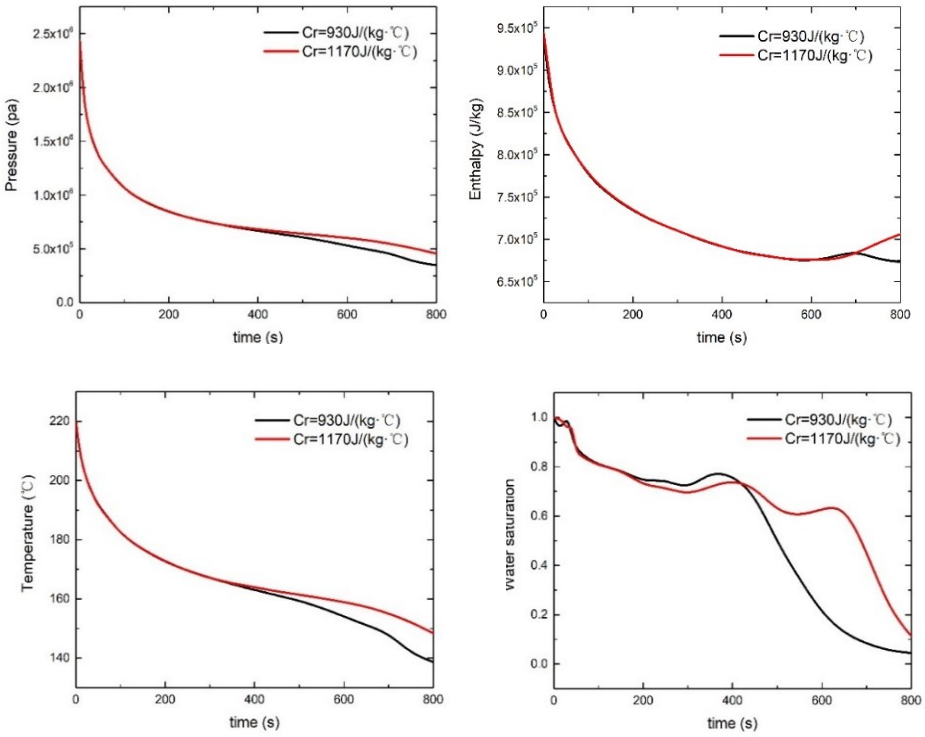

Figure 10 Pressure, enthalpy, temperature and water saturation with different rock heat capacity

7. CONCULSION

A numerical model is developed for describing multiphase flow in porous media based on pressure and enthalpy. The latest IAPWS Industry Formulation 1997 is used here as precise algorithms for calculating fluid thermodynamic properties in both water and water-steam region. The nonlinearities and slope discontinuities in the seven coefficients of governing equations which cause a major convergence difficulty are presented in great details. Newton-Raphson, automatic time step size control method and three convergence criteria are used here to ensure numerical convergent solution.

This model of this paper is used to simulate the sudden pressure drop in geothermal process. The numerical results suggest that the sudden pressure drop can induce phase change in the porous medium and the thermophysical rock properties will affect the water steam phase change behavior. By comparing pressure, temperature, enthalpy and water saturation profiles, it can be concluded that heat transfer by fluid flow is the dominating factor in the thermal process, since the factor that can effect pressure evolution significantly has a great influence on enthalpy, and further influence temperature and water saturation evolution. Further research is required to understand how fluid flow and heat transfer process interact with each other and further extended to simulate geothermal flow with the consideration of gravity to get the more reliable and realistic solution.

REFERENCES

Bergins, C., et al. (2005). "Multiphase flow in porous media with phase change. Part II: Analytical solutions and experimental verification for constant pressure steam injection." 60(3): 275-300.

Coats, K., et al. (1974). "Three-dimensional simulation of steamflooding." 14(06): 573-592.

Corey, A. T. J. P. m. (1954). "The interrelation between gas and oil relative permeabilities." 19(1): 38-41.

Croucher, A., et al. (2016). Geothermal Supermodels Project: an update on flow simulator development. Proceedings 38th New Zealand Geothermal Workshop.

Croucher, A., et al. (2018). Benchmarking and experiments with Waiwera, a new geothermal simulator. Proceedings, 43rd Workshop on Geothermal Reservoir Engineering. Stanford University, Stanford, California.

Doughty, C., et al. (1988). "A semianalytical solution for heat-pipe effects near high-level nuclear waste packages buried in partially saturated geological media." 31(1): 79-90.

Faust, C. R. (1976). "Numerical simulation of fluid flow and energy transport in liquid-and vapor-dominated hydrothermal systems."

Faust, C. R. and J. W. J. W. r. r. Mercer (1979). "Geothermal reservoir simulation: 1. Mathematical models for liquid‐and vapor‐dominated hydrothermal systems." 15(1): 23-30.

Garg, S., et al. (1975). "Simulation of fluid-rock interactions in a geothermal basin."

Garg, S., et al. (1978). "Geopressured geothermal reservoir and wellbore simulation."

Gudjonsdottir, M., et al. (2015). "Calculation of relative permeabilities of water and steam from laboratory measurements." Geothermics 53: 396-405.

Horne, R. N. and M. J. O'Sullivan (1977). Numerical Modeling Of The Wairakei Geothermal Reservoir. SPE California Regional Meeting, Society of Petroleum Engineers.

Horne, R. N., et al. (2000). "Steam-water relative permeability." 597-604.

Mannington, W., et al. (2004). "Computer modelling of the Wairakei–Tauhara geothermal system, New Zealand." 33(4): 401-419.

Melaku, M. (2005). Geothermal development at Lihir–an overview. Proceedings of World Geothermal Congress.

O'Sullivan, M. J. J. W. R. R. (1981). "A similarity method for geothermal well test analysis." 17(2): 390-398.

Pruess, K. and T. Narasimhan (1982). "A practical method for modeling fluid and heat flow in fractured porous media."

Sass, I. and A. E. J. T. N. Götz (2012). "Geothermal reservoir characterization: a thermofacies concept." 24(2): 142-147.

Shaik, A. R., et al. (2011). "Numerical simulation of fluid-rock coupling heat transfer in naturally fractured geothermal system." 31(10): 1600-1606.

Singh, M. (2010). Management of Geohazards at Lihir Gold Mine-Papua New Guinea, University of Alberta.

Thomas, L. K. and R. G. J. S. o. P. E. J. Pierson (1978). "Three-dimensional geothermal reservoir simulation." 18(02): 151-161.

Voss, C. I. (1979). "Finite element simulation of multiphase geothermal reservoirs."

Wagner, W. and H.-J. Kretzschmar (2007). International Steam Tables-Properties of Water and Steam based on the Industrial Formulation IAPWS-IF97: Tables, Algorithms, Diagrams, and CD-ROM Electronic Steam Tables-All of the equations of IAPWS-IF97 including a complete set of supplementary backward equations for fast calculations of heat cycles, boilers, and steam turbines, Springer Science & Business Media.

Witherspoon, P., et al. (1975). "Modeling geothermal systems."

Xing, H. J. J. o. G. E. (2014). "Finite element simulation of transient geothermal flow in extremely heterogeneous fractured porous media." 144: 168-178.

Zalba, B., et al. (2003). "Review on thermal energy storage with phase change: materials, heat transfer analysis and applications." 23(3): 251-283.

Zyvoloski, G. A., et al. (1997). Summary of the models and methods for the FEHM application-a finite-element heat-and mass-transfer code, Los Alamos National Lab., NM (US).